

Article

Prediction of Potential Habitats of *Zanthoxylum armatum* DC. and Their Changes under Climate Change

Pingping Tian ¹, Yifu Liu ², Mingzhen Sui ¹ and Jing Ou ^{1,*}¹ College of Forestry, Guizhou University, Guiyang 550025, China² Ecology and Nature Conservation Institute, Chinese Academy of Forestry, Beijing 100091, China

* Correspondence: coloroj@126.com; Tel.: +86-1398-4184-857

Abstract: Climate change poses a severe threat to biodiversity. Greenhouse gas emissions have accelerated climate warming and significantly impacted species distribution and population dynamics. *Zanthoxylum armatum* DC. is an ecologically, medicinally, and economically important plant; it is cultivated as an economic crop at large scales in China, and is a valuable medicinal plant in India, Nepal, etc. A precise prediction of the potential distribution areas of *Z. armatum* will contribute to its protection and determination of its planting areas. In this paper, based on 433 distribution points and 19 climate factors, the MaxEnt model was used to analyze the spatial distribution pattern of *Z. armatum* between 1970 and 2000, predict its spatial distribution pattern in 2040–2060 (the 2050s) and 2081–2100 (the 2090s), and comprehensively assess the critical climate factors limiting its geographical distribution. The findings are as follows: (1) in the 1970–2000 scenario, the potential suitable distribution areas of *Z. armatum* include the subtropical monsoon climate regions of Japan, the Korean Peninsula, the south of the Qinling–Huaihe Line of China, and the regions along the southern foot of the Himalayas (India, Bhutan, Nepal, etc.), with an area of 330.54×10^4 km²; (2) the critical climate factors affecting the potential distribution of *Z. armatum* include temperature (mean diurnal temperature range, mean temperature of the coldest quarter, and temperature seasonality) and annual precipitation; (3) the distribution areas of *Z. armatum* will shift to higher latitudes and shrink under the three climate change scenarios in the 2050s and 2090s. In the 2090s–SSP585 scenario, the total area of suitable habitat will decrease most markedly, and the decrease rate of the highly suitable areas will reach up to 97.61%; only the region near Delong Town, Nanshan District, Chongqing City, will remain a highly suitable habitat, covering an area of merely 0.08×10^4 km². These findings suggest that *Z. armatum* is susceptible to climate change. The border area between Guizhou Province and Chongqing City and the southwest district of Leshan City, Sichuan Province, will be a stable and moderately high potential suitable habitat for *Z. armatum* in the future. The above regions are recommended to be managed as key protected areas.

Keywords: *Zanthoxylum armatum* DC.; climate change; climate factors; suitable area

Citation: Tian, P.; Liu, Y.; Sui, M.; Ou, J. Prediction of Potential Habitats of *Zanthoxylum armatum* DC. and Their Changes under Climate Change. *Sustainability* **2022**, *14*, 12422. <https://doi.org/10.3390/su141912422>

Academic Editors: Dong Kook Woo, Yongwon Seo and Esther Lee

Received: 22 August 2022

Accepted: 26 September 2022

Published: 29 September 2022

Publisher's Note: MDPI stays neutral with regard to jurisdictional claims in published maps and institutional affiliations.



Copyright: © 2022 by the authors. Licensee MDPI, Basel, Switzerland. This article is an open access article distributed under the terms and conditions of the Creative Commons Attribution (CC BY) license (<https://creativecommons.org/licenses/by/4.0/>).

1. Introduction

The Intergovernmental Panel on Climate Change (IPCC) argues that, at present, the global average surface temperature is 1.09 °C higher than that in 1850–1900, and global climate change will intensify in the next few decades [1]. Climate change is an external driving factor affecting the distribution, population size, reproduction, and migration of species [2]. Under the influence of climate change, biogeographic distributions show dynamic changes in time and space [3,4]. By climate simulation using eight general circulation models (GCMs), certain spatial vegetation patterns were observed; specifically, the high-latitude northern forest expanded to the polar region, and the tropical vegetation types significantly degraded [5]. In the future, global climate change will become the most significant factor influencing biodiversity and population diversity [6].

The prediction of niche and potential suitable areas for specific organisms under climate change is a research focus in ecology and biogeography [7,8]. Species distribution models (SDMs) can associate the known living areas of organisms with environmental factors and foresee their potential living areas [9]. At present, many climate change-based modeling methods are accessible for species distribution prediction, such as Bioclim, GAM, GLM, GARP, and MaxEnt [10,11]. An appropriate one should be selected to avoid deviation from the prediction results [12]. The MaxEnt model shows optimum performance in terms of overall software utility and has been widely used [10]. Since 2006, the MaxEnt model has been used in more than 1000 published applications to predict the potential distribution areas of rare and endangered economic and medicinal species worldwide [13], to assess their extinction risk [14]. For example, Ye et al. [15] and Tan et al. [16] utilized the MaxEnt model to predict the potential geographical distribution of the endangered plant *Davidia involucreata* and medicinal plant *Gentiana macrophylla* under climate change in China. Moreover, they put forward protection strategies according to the prediction results. Feng et al. [17] employed the MaxEnt model to predict the change in potential planting areas of soybean in the world under climate change. The prediction of the potential living areas of various species under different climate scenarios is critical for the protection of germplasm resources of critical species.

Zanthoxylum armatum, in the genus *Zanthoxylum* (Rutaceae), is a small tree or shrub with high ecological, medicinal, and economic value. It is mainly distributed in China, Japan, Korea, Vietnam, Laos, Myanmar, India, Nepal, etc. [18–20]. *Z. armatum* has been cultivated in China for a long time, with a planting area of 108.76 hectares, an annual output of 374,000 tons, and an annual output value of more than USD 40 billion. The planting area and output of *Z. armatum* in China rank first in the world. It is one of the crucial cash crops in China [21–23]. The National Forestry and Grassland Administration of China has taken *Z. armatum* as a key tree species to plant in national economic forests in the Forest and Grass Industry Development Plan (2021–2025). In India, Nepal, and other South Asian countries, *Z. armatum* is a medicinal plant important for economic development. Due to climate change and over-exploitation, the wild population of *Z. armatum* has declined rapidly, and *Z. armatum* has been listed as an endangered species in the Himalayas region of India [20,24,25]. The current research on *Z. armatum* mainly focuses on physiology, cultivation techniques, and chemical components. Research on the genetic diversity of *Z. armatum* germplasm shows that a large proportion of the wild population of *Zanthoxylum bungeanum* has gradually disappeared or been replaced by the cultivated population [26–29]. The genetic diversity of *Z. bungeanum* in China was studied based on the GBS approach, and it was found that the genetic diversity of *Z. armatum* was much lower than that of *Z. bungeanum* [25]. These studies provide a certain basis for the protection of germplasm resources and the wild population of *Z. armatum*. However, at present, studies on the dynamic changes and protection of wild *Z. armatum* under future climate conditions are rare. In this paper, the MaxEnt model was used to simulate the impact of climate change on the potential spatial distribution pattern of *Z. armatum* and reveal the changes in *Z. armatum* distribution area in the future. In addition, the MaxEnt model was applied to identify the key climate factors affecting the distribution and potential risk factors of *Z. armatum* extinction. It is expected that this paper can provide a scientific basis for the protection of germplasm resources of *Z. bungeanum* and the regional planning of its artificial cultivation and contribute to the sustainable utilization of *Z. armatum* resources.

2. Materials and Methods

2.1. Species Distribution Point Data

The data on the natural distribution points of *Z. armatum* were collected on 15 November 2021 by visiting by accessed the Global Biodiversity Information Facility (GBIF, <https://www.gbif.org/>), Chinese Virtual Herbarium (CVH, <http://www.cvh.ac.cn/>), National Specimen Information Infrastructure of China (NSII, <http://www.Nsii.org.cn>), and published literature. A total of 466 original wild distribution points were obtained. To

avoid geographic autocorrelation of the distribution locations, ENMTools V1.4 was utilized for the screening of redundant data. Finally, 433 effective natural distribution points of *Z. armatum* were obtained (Figure 1).

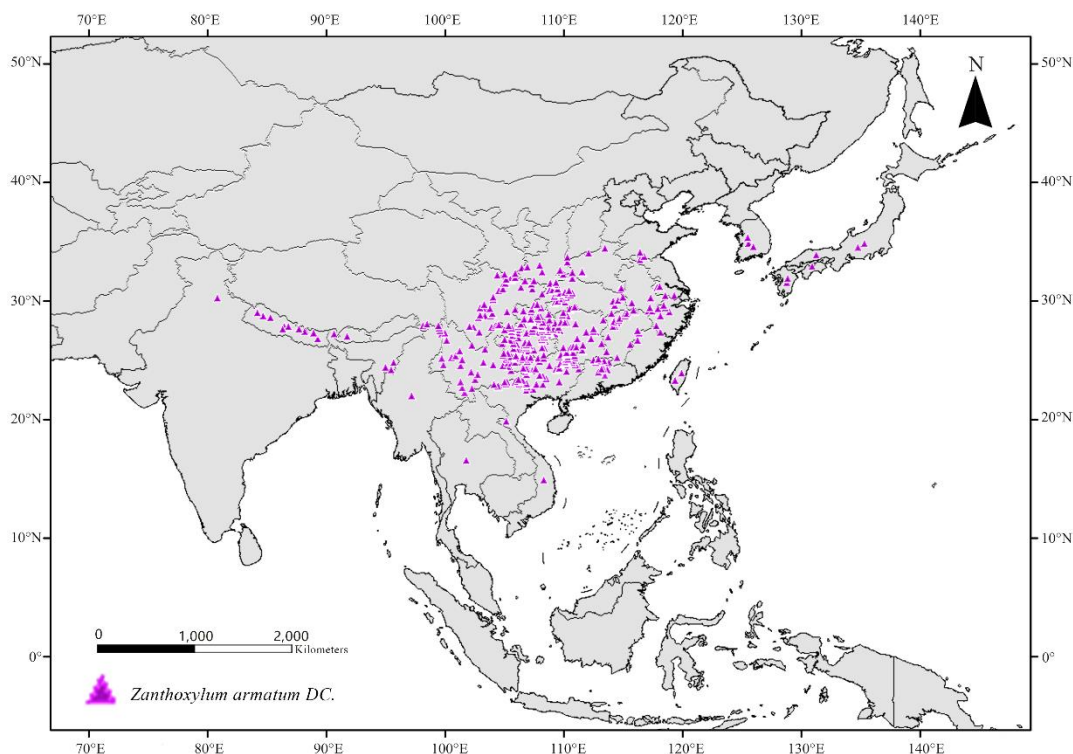


Figure 1. Geographical distribution points of *Z. armatum*.

2.2. Environmental Variables

In this research, variables related to the 19 global climate factors with a geographic resolution of 2.5 arc min in three periods, i.e., 1970–2000, 2041–2060 (the 2050s), and 2081–2100 (the 2090s), were obtained on 10 January 2022 by visiting by accessed the World Climate Data website (www.worldclim.org). Two atmospheric circulation models, namely, BCC-CSM2-MR and MRI-ESM2-0 in CMIP6, were selected [30], in which three shared socioeconomic paths, namely, sustainable path (SSP126), middle path (SSP245), and fossil fuel-based development path (SSP585), were chosen to increase the reliability of climate data [31,32]. Based on the distribution areas of *Z. armatum*, R v3.6.2 software was employed to cut the climate data and convert them to the “.asc” format.

The data of 19 climatic parameters at each location were extracted using the “Extract Multi Values to Points” feature of the Arcgis10.2 program [16]. Then, the Pearson correlation coefficient matrix between the corresponding climate factors at each point was calculated with R v3.6.2 to determine their significant correlation with 0.8 as the threshold.

After screening, the data on 433 effective natural distribution points and 19 climate factors between 1970 and 2000 were imported into MaxEnt3.4.1 for a four-time operation. The results were analyzed by comparing the percent contribution and Jackknife values; climate factors with a contribution rate of less than 0.5 were deleted. The relatively most important one of the two significant correlation factors was retained. Finally, eight climate factors were obtained from 19 climate factors for modeling (Table 1).

Table 1. Contribution rate and permutation importance of the climate factors.

Climate Factor	Description	Percent Contribution (%)	Permutation Importance (%)
BIO02	Mean diurnal temperature range (Mean of monthly (max temp-min temp)) ($^{\circ}\text{C} \times 10$)	43.9	21.5
BIO11	Mean temperature of coldest quarter ($^{\circ}\text{C} \times 10$)	38.6	34.9
BIO04	Temperature seasonality (standard deviation $\times 100$)	12.5	5.4
BIO14	Precipitation of driest month (mm)	2.2	7.1
BIO12	Annual precipitation (mm)	1.4	19
BIO08	Mean temperature of wettest quarter ($^{\circ}\text{C} \times 10$)	0.6	2.6
BIO15	Precipitation seasonality (coefficient of variation) (mm)	0.4	7.9
BIO18	Precipitation of warmest quarter (mm)	0.3	1.7

2.3. Model Building

MaxEnt comprises five features, namely, L = linear, Q = quadratic, P = product, T = threshold, and H = hinge. Because the H = hinge feature was introduced later than the T feature, it was used as an alternative to the T feature rather than a supplement [33]. The T feature was ignored in this study. The *Kuerm* package in Rv3.6.1 was used to provide the judgment standard of the optimal model. Specifically, 15 combinations of 4 element types were considered, and 40 regularization multipliers (RM) were set at an interval of 0.1 to form 600 parameter combinations. The parameter combinations were evaluated and modeled, by which the optimization of feature type FC and RM was achieved. Then the optimum model for modeling was selected according to the following criteria: (1) significance and omission rate ($E < 0.05$); and (2) model complexity AICc ($\text{delta} \leq 2$) [34]. Finally, two element types were sifted out, namely, the Q and P features, and RM was 0.2.

Subsequently, the data of 433 *Z. armatum* natural distribution points and filtered climate factors were imported into MaxEnt software. Q and P features were selected in the element-type part, while the subsample was chosen in the replicated run-type part. The modeling was repeated ten times, and its RM was 0.2. A test set made up of 30% of the distribution data was chosen, with the remaining 70% serving as the training set. In order to ensure sufficient time for the model to achieve convergence, the maximum iteration was set to 5000 times. After modeling by MaxEnt v3.4.1, the Jackknife method was used to test the weight based on the percent contribution of the selected climate factors. The receiver operating characteristic (ROC) curve was plotted. The accuracy of the simulation results was evaluated based on the area under the curve (AUC), since AUC, unlike AUCTRAN, is seldom influenced by overfitting, and training data overfitting does not necessarily improve the fitting of independent test data [35]. The AUC value varied from 0 to 1, with larger values indicating better prediction accuracy. An AUC value < 0.6 means failure; 0.6–0.7 indicates poor prediction accuracy; 0.7–0.8 implies fair prediction accuracy; 0.8–0.9 represents good prediction accuracy; 0.9–1.0 indicates excellent prediction accuracy [36,37].

Based on the modeling results, Arcgis10.2 was used to visualize the prediction map of potential distribution regions in 1970–2000, the 2050s, and the 2090s, and the areas of suitable distribution regions were calculated. Generally, the most accurate predictions were made based on the “sensitivity-specificity difference minimizer” and “sensitivity-specificity sum maximizer” criteria. Therefore, in this study, the maximum training sensitivity plus specificity threshold of 0.1227 generated by MaxEnt was selected as the threshold to determine whether a region is suitable for *Z. armatum* [38]. The potential distribution regions were classified as follows: unsuitable region ($p < 0.1227$), lowly suitable region ($0.1227 \leq p < 0.4151$), moderately suitable region ($0.4151 \leq p < 0.7076$), and highly suitable region ($p \geq 0.7076$).

3. Results

3.1. Evaluation of Model Prediction Accuracy

According to the projection of the potential suitable distribution regions of *Z. armatum* by the MaxEnt model, the average AUC value was 0.953 (Figure 2), indicating the excellent accuracy of the model. It can be concluded that the MaxEnt model is appropriate for the simulation of potential distribution areas of *Z. armatum* under the climate scenarios in 1970–2000, the 2050s, and the 2090s.

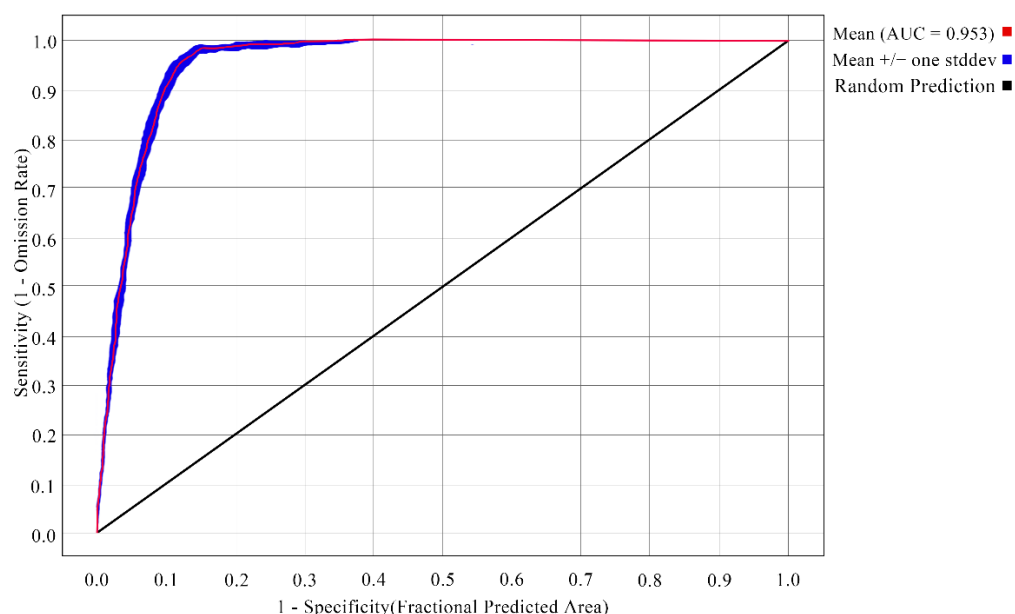


Figure 2. Test of the ROC generated by the MaxEnt model.

3.2. Critical Climate Factors Affecting the Geographical Distribution of *Z. armatum*

As seen in Table 1, BIO02 and BIO11 exerted the greatest impact on *Z. armatum*. The percent contribution and permutation importance of BIO02 were 43.9% and 21.5%, respectively, while those of BIO11 were 38.6% and 34.9%, respectively. According to the importance assessment of climate factors related to *Z. armatum* distribution by Jackknife (Figure 3), the test gain was the highest when there was only BIO02; the test gain was the second highest when there was only BIO11; the test gain ranked third when there was only BIO04, indicating that the three factors were the most important ones. Moreover, the gain of BIO18 was the smallest, indicating that it is the least important factor for the prediction of *Z. armatum* geographical distribution. When BIO02 and BIO12 were ignored, the overall gain became smaller, proving the two factors contained exclusive information. In summary, the principal climatic elements impacting *Z. armatum* distribution were BIO02, BIO11, BIO04, and BIO12.

Figure 4 shows the response curves of *Z. armatum*. These curves show how each environmental variable affects the MaxEnt prediction. It can be seen that BIO12 and BIO04 exerted the most marked effect on the future distribution of bamboo leaf peppercorns. When BIO12 was 2.63 °C, BIO04 was 55.53 °C, BIO11 was 4.57 °C, and BIO12 was 1076.62 mm; also, *Z. armatum* grows best, and its distribution range is the largest.

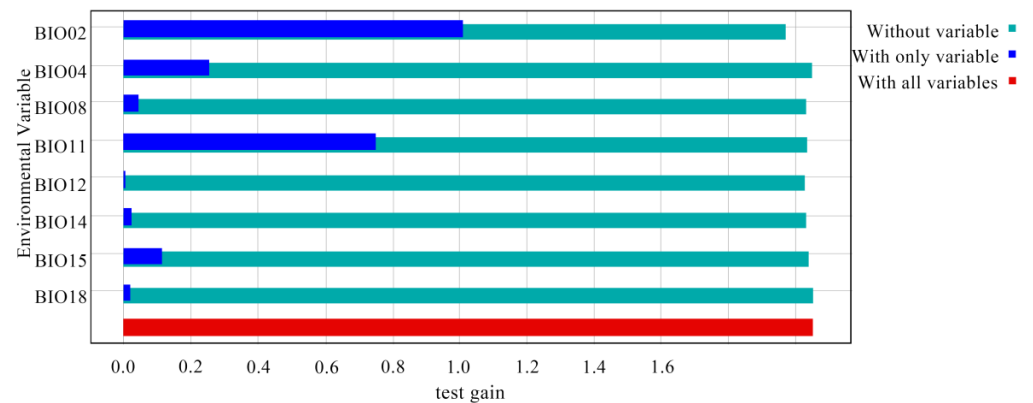


Figure 3. Evaluation of the relative significance of the leading environmental factors for *Z. armatum* using the Jackknife of test gain. The contribution rate and permutation significance of the related climatic variables are shown in Table 1.

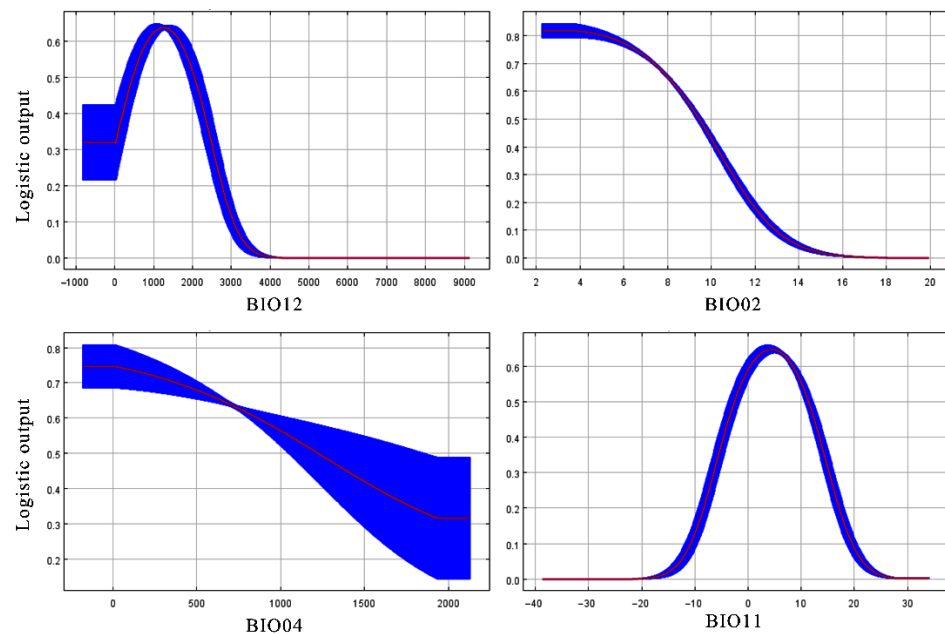


Figure 4. Response curves of *Z. armatum* show how the predicted probability of presence changes as each environmental variable is varied; the response is the mean (red) \pm standard deviation (blue).

3.3. Distribution of Potential Suitable Areas of *Z. armatum* in 1970–2000

Based on the simulation by the MaxEnt model, the potential distribution areas of *Z. armatum* under the climate scenario in 1970–2000 are mainly located in China, Vietnam, Laos, Myanmar, Kyrgyzstan, Tajikistan, Pakistan, North Korea, South Korea, and Japan; moreover, *Z. armatum* is also distributed in the southern foothills of the Himalayas (India, Bhutan, Nepal, and southern Tibet of China). The above potential areas are wider than the current distribution points (Figure 5). The entire area of the distribution regions is $3.30 \times 10^6 \text{ km}^2$. The highly suitable regions are mainly in Sichuan Province, Chongqing City, and Guizhou Province of China, with an area as small as $3.56 \times 10^4 \text{ km}^2$ (1.08% of the total); the moderately suitable regions are mainly in the southwest of China, covering an area of $1.49 \times 10^6 \text{ km}^2$ (45.14% of the total); the lowly suitable regions cover an area of $1.78 \times 10^6 \text{ km}^2$ (53.79% of the total).

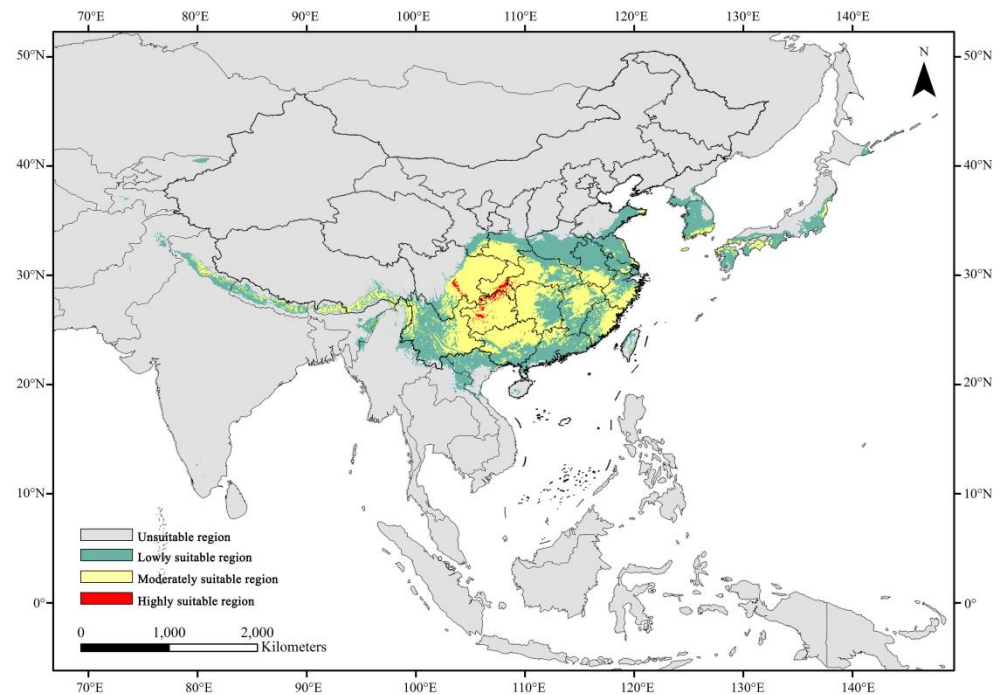


Figure 5. Potential distribution areas of *Z. armatum* under climate conditions in 1970–2000.

3.4. Potential Suitable Areas of *Z. armatum* under Future Climate Scenarios

Under the three climate scenarios, namely, SSP126, SSP245, and SSP585, in the 2050s, the overall suitable regions for *Z. armatum* will present a decreasing trend (Figures 6 and 7); it will reduce $7.61 \times 10^4 \text{ km}^2$, $2.03 \times 10^4 \text{ km}^2$, and $5.00 \times 10^4 \text{ km}^2$, respectively. The lowly suitable regions will increase by $4.70 \times 10^5 \text{ km}^2$, $3.51 \times 10^5 \text{ km}^2$, and $4.52 \times 10^5 \text{ km}^2$, respectively; in contrast, the moderately and highly suitable regions will decrease. The moderately suitable regions will be reduced by $5.12 \times 10^5 \text{ km}^2$, $2.99 \times 10^5 \text{ km}^2$, and $4.68 \times 10^5 \text{ km}^2$, respectively, and the highly suitable regions will be reduced by $3.36 \times 10^4 \text{ km}^2$, $3.12 \times 10^4 \text{ km}^2$, and $3.30 \times 10^4 \text{ km}^2$, respectively. Under the SSP585 scenario in particular, the highly suitable regions can only be found between the border of Chongqing City and Guizhou Province, covering an area of merely $1.94 \times 10^3 \text{ km}^2$.

The overall suitable areas will shrink under the three 2090s climatic scenarios, namely, SSP126, SSP245, and SSP585; it will reduce to $1.02 \times 10^5 \text{ km}^2$, $7.71 \times 10^4 \text{ km}^2$, and $3.26 \times 10^5 \text{ km}^2$, respectively. The lowly suitable regions will expand $2.83 \times 10^5 \text{ km}^2$, $4.86 \times 10^5 \text{ km}^2$, and $7.29 \times 10^5 \text{ km}^2$, respectively, shifting to higher latitudes. The moderately suitable regions will shrink $3.55 \times 10^5 \text{ km}^2$, $5.29 \times 10^5 \text{ km}^2$, and $1.02 \times 10^6 \text{ km}^2$, respectively. Under the SSP585 scenario, the area of moderately suitable regions will be reduced to $4.7 \times 10^5 \text{ km}^2$, and they will only be located in the center of Sichuan, northwest Guizhou, southeast Chongqing, southwest Hubei, southern Shaanxi, northern Jiangxi, southern Anhui, eastern and western Zhejiang, and the hot regions of the Himalayas (Yunnan, Myanmar, Tibet, Bhutan, Nepal, India, etc.), as well as small parts of South Korea, North Korea, and Japan. The decreasing trend of highly suitable regions in the 2090s is more intense than that in the 2050s, with $3.02 \times 10^4 \text{ km}^2$, $3.35 \times 10^4 \text{ km}^2$, and $3.47 \times 10^4 \text{ km}^2$ reduced, respectively. Under the SSP585 scenario, the area of highly suitable regions will drop to $8 \times 10^2 \text{ km}^2$, covering only 0.03% of the total. They will only be located in the southern border area of Chongqing in China; in other words, the highly suitable regions will almost disappear.

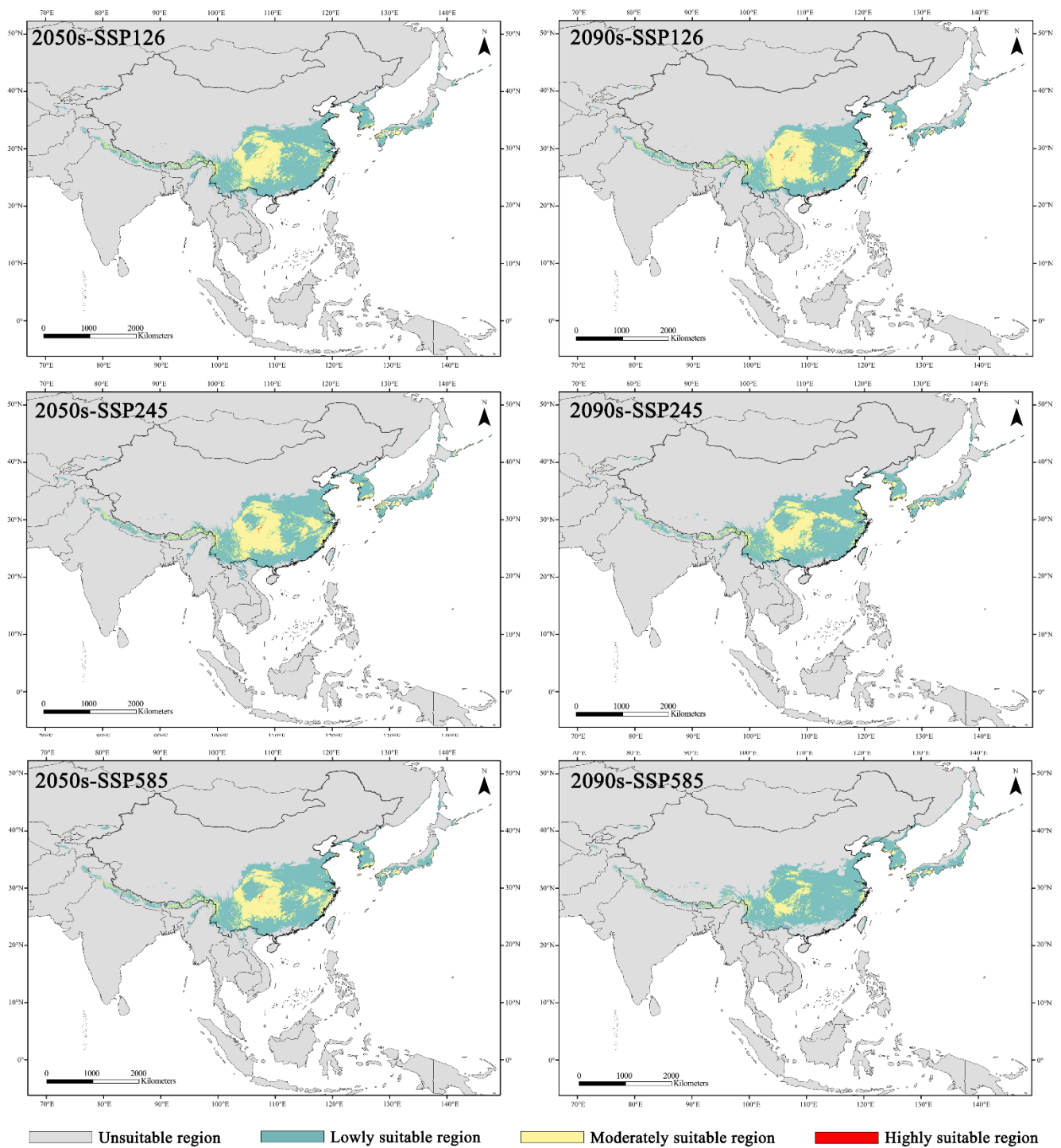


Figure 6. Potential distribution range of *Z. armatum* under the 2050s and 2090s climatic scenarios.

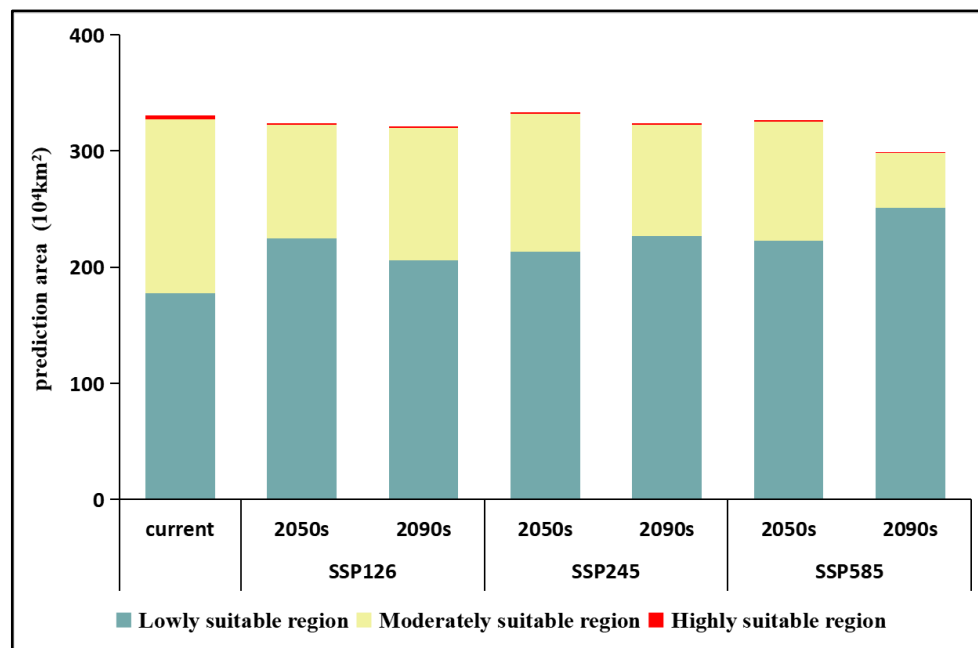


Figure 7. Prediction of *Z. armatum* suitable areas under climate scenarios in 1970–2000, the 2050s, and the 2090s.

4. Discussion

4.1. Important Climate Variables influencing Potential Distribution of *Z. armatum*

Based on the MaxEnt model, the suitable distribution areas of *Z. armatum* in 1970–2000, the 2050s, and the 2090s were predicted. The AUC value was 0.953, and thus higher than 0.9, indicating the excellent prediction accuracy and high reliability of the model [36,37]. Feng et al. [26] performed GBS sequencing research. They found that the southwest mountainous area of China might be home to *Z. armatum*, which was considered a refuge during the peak of the last glacial period. *Z. armatum* began to migrate outward during the interglacial period. The model simulation results showed that the main potential distribution areas of *Z. armatum* in 1970–2000 include the subtropical monsoon climate areas of Japan, the south of the Qinling–Huaihe Line in China, and the Korean Peninsula, as well as the areas along the southern foot of Himalayas (India, Bhutan, Nepal, etc.). The most highly suitable regions are in Sichuan and Guizhou in southwest China. These findings are in line with those in previous studies [26,39] and the record in *Flora of China* [19]. The model results are consistent with the actual growth characteristics of *Z. armatum*.

As screened by MaxEnt modeling, the importance of the critical climate factors affecting *Z. armatum* distribution followed the order of BIO02 > BIO11 > BIO04 > BIO12. When BIO02 is 2.63 °C and BIO04 is 55.525 °C, the growth vigor of *Z. armatum* is the best. With the increase in temperature difference, the adaptability of *Z. armatum* continues to decrease. When BIO11 is 4.57 °C, the *Z. armatum* fitness is optimal and decreases with the increase in BIO11, indicating that excessively high or low temperature will impede *Z. armatum* growth. When BIO12 is 1076.62 mm, *Z. armatum* has the best adaptability, which also explains the reason why highly suitable regions for *Z. armatum* are mainly distributed in the Sichuan and Guizhou regions of Southwest China. Xu et al. [39] believed that the principal climatic variables influencing the distribution of *Z. armatum* were the relevant temperatures in January, February, and March; the precipitation in July; and the average temperature and average annual precipitation in the coldest quarter. *Z. armatum* is mainly distributed in the south of the Qinling–Huaihe Line. This region is affected by a subtropical monsoon climate characterized by abundant heat and precipitation, which provide suitable conditions for the growth of *Z. armatum* [40]. Moreover, in China, the coldest season is from December to February of the next year, during which the growth of *Z. armatum* is significantly impacted by temperature. In winter, *Z. armatum* stops

growing; the leaves fall, and buds are in a dormant state. When the temperature rises in spring, it enters a slow growth period; i.e., the ovary differentiation stage. Then, the young leaves outside the flower bud begin to unfold, the light green inflorescences are exposed at the bud top, and the inflorescences are drawn out, which marks the end of the bud stage. The spring temperature in the south of the Qinling–Huaihe Line in China is suitable for the dormancy release of *Z. armatum* [41,42]. In addition, the cold resistance of *Z. armatum* is weakened below 0 °C. The flower buds and leaf buds of *Z. armatum* are bare and tend to sustain freezing damage at excessively low average temperatures in winter [43]. *Z. armatum* likes water and fertilizer but can easily die of water accumulation; thus, the precipitation will also significantly impact its growth and development [44]. The warm and humid airflow of the Indian Ocean brings abundant rainfall to the southern foothills of the Himalayas, making them suitable regions for the growth of *Z. armatum* [45]. In summary, BIO02, BIO11, BIO04, and BIO12 are the critical climate factors influencing the growth of *Z. armatum* and its potential distribution in the future.

4.2. Future Change in the Potential Distribution of *Z. armatum*

By predicting the potential suitable distribution regions of *Z. armatum* given the current and future climate, it was found that the subtropical monsoon humid climate provides the most suitable conditions for *Z. armatum*, and both supercooling and overheating may impede the growth of *Z. armatum*. According to the model prediction of previous studies, global warming is still a serious issue in 2040; the middle and high latitudes of Asia will show an exceptional warming trend, and the cold events will continue to drop. By 2090, the temperature will rise most dramatically under the SSP585 scenario, by about 7–10 °C. Moreover, the future precipitation will also show an increasing trend in the north and a decreasing trend in the south. The precipitation in high latitude zones in the warm season will be enhanced slightly, while that in the cold season will increase by about 10–40% [46]. The high latitude regions in the north of the existing range will become suitable for *Z. armatum* growth due to future climate change. Under the six scenarios in the future, the distribution range of *Z. armatum* may shift to higher latitudes. The modeling results show that with the social economy being more complex and the radiation degree becoming higher than before, the migration trend to higher latitudes will be more significant, and the suitable regions will be more fragmented, especially under the SSP585 scenario in the 2050s and 2090s.

The suitable areas of *Z. armatum* will shrink due to future climate change. Under the 2090s–SSP585 scenario, the total area of suitable regions will be reduced from $330.54 \times 10^4 \text{ km}^2$ to $297.93 \times 10^4 \text{ km}^2$ at a decrement rate of 9.87%. Under the 2090s–SSP585 scenario, the total area of suitable regions will decrease most markedly at a decrement rate of 9.87%. Guangxi, southern Guangdong, and Hainan in China, as well as southern India, will become unsuitable for the growth of *Z. armatum*; in contrast, suitable areas in Tibet, Gansu, Shaanxi, Henan, and Shandong in China will increase, which indicates that the potential distribution of *Z. armatum* may be impacted by climate change, and the impact will intensify with the increase in radiation degree. Previous research has shown that the temperature in the north of the Qinling–Huaihe Line in China will increase, and future climate change under RCP8.5 is more dramatic than that under RCP4.5. Generally, the area of arid regions will increase while that of humid regions will decrease, which may explain the future decrease in suitable habitats for *Z. armatum* [47,48]. Under the climate scenario in 1970–2000, the area of highly suitable regions is predicted to be $3.56 \times 10^4 \text{ km}^2$, and they are mainly in the border region between Guizhou Province and Chongqing City, and the southwest districts and counties of Leshan City, Sichuan Province. Under the six future climate scenarios, the highly suitable regions will be reduced. Particularly under 2090s–SSP585, the area will decrease by $3.48 \times 10^4 \text{ km}^2$, with a decline rate of 97.61%. They will only be located near Delong Town, Nanshan District, Chongqing City, with an area of merely $0.08 \times 10^4 \text{ km}^2$. In addition, the potential moderately suitable regions will be greatly reduced in southwest China, and the regions will also present a high degree of fragmentation. Moderately and highly suitable regions are transformed into

lowly suitable regions, and therefore, lowly suitable regions generally show an increasing trend. In conclusion, future climate change may cause the moderately or highly suitable regions for *Z. armatum* to become less suitable or even non-suitable regions, with an enhanced radiation intensity.

4.3. *Z. armatum* Protective Strategy

The suitable distribution areas of *Z. armatum* have shrunk slightly since the middle Holocene [26]. The present study shows that with future climate change becoming more and more severe, suitable distribution areas of *Z. armatum* will further decrease, and the highly suitable areas will almost disappear. As a high-quality seasoning and traditional Chinese medicine, *Z. armatum* will be cultivated on a larger scale. However, in the future, the reduction in suitable areas, especially highly suitable areas, will lead to the loss of the wild *Z. armatum* population, thus reducing the genetic diversity of *Z. armatum* and increasing the difficulty of breeding excellent varieties, which will bring a series of adverse effects. For example, the planting yield of *Z. armatum* will be significantly reduced, and its quality will be degraded, which will influence the pepper industry in China, India, Nepal, etc. Scientific protective strategies should be adopted for sustainable utilization of *Z. armatum* resources. First, the model prediction revealed the stable and suitable areas for *Z. armatum* are mainly in central Sichuan, northwest Guizhou, southeast Chongqing, southwest Hubei, and south Shaanxi in China, especially the border area between Guizhou and Chongqing and southwest Leshan, Sichuan. These regions can be set as priority protection areas of the wild germplasm resources of *Z. armatum*. At the same time, artificial planting technology can be implemented, and a wild nursery can be established for *Z. Armatum* to provide suitable conditions for its growth and maintain minimum viable populations [49,50]. Second, a gene bank can be built to preserve wild *Z. armatum* resources in moderately and highly suitable areas that will disappear in the future through in vitro culture or low-temperature preservation. In this way, the genetic diversity of *Z. armatum* can be protected, and the exchange of global *Z. armatum* germplasm resources will be strengthened [51]. Third, it is necessary to strengthen the research on the selection and breeding of excellent *Z. armatum* varieties to improve the stress resistance, such as cold resistance, heat resistance, and waterlogging resistance, increase the edible and medicinal value, and expand the cultivation yield of artificially cultivated varieties within the scope of potential suitable areas. It is worth noting that the prediction results of the MaxEnt model may deviate from the actual situation, despite its high prediction accuracy. The possible reasons are as follows. Firstly, in this study, the adaptive evolution of *Z. armatum* in response to future climate change and its adaptive range expansion through measures such as variety improvement are not considered. Secondly, soil conditions, biological relationships, and human activities all affect the distribution of plants, in addition to climatic factors. Thirdly, the data used in this study are from the WorldClim database. The time span from 2000 to the 2090s is large. The improvement in future cultivation technology and the intensification of *Z. armatum* protection may also contribute to the increase in suitable areas of *Z. armatum*. Despite the above limitations, the model is still of guiding significance for natural resource protection and artificial planting of *Z. armatum*, since it is difficult to incorporate all elements into a specific model, and the geographical distribution of plants on a regional scale is mainly restricted by climate factors [52].

5. Conclusions

The potential distribution of *Z. armatum* is mainly influenced by four critical climatic factors: mean diurnal temperature range, mean temperature of coldest quarter, temperature seasonality, and annual precipitation. The potential suitable distribution areas of *Z. armatum* in 1970–2000 are the subtropical monsoon climate areas of Japan, the Korean Peninsula, the south of the Qinling–Huaihe Line of China, and the areas along the southern foot of the Himalayas. The distribution range of *Z. armatum* in the 2050s and 2090s tends to shift to higher latitudes under the three possible future climatic scenarios, and the area of

suitable regions will decrease. Under the 2090s–SSP585 scenario, the suitable regions will shrink most dramatically. The southwest district of Leshan City, Sichuan Province, and the border area between Guizhou Province and Chongqing City potentially will be stable and moderately to highly suitable regions for *Z. armatum* in the future. The above regions are recommended to be managed as key protected areas. Considering wild *Z. armatum* in the moderately and highly suitable areas that will disappear in the future, the genetic diversity should be preserved through field gene banks and other ways, and research on the selection and breeding of excellent varieties should be strengthened.

Author Contributions: P.T. and Y.L.; methodology, P.T.; software, P.T.; validation, P.T. and Y.L.; formal analysis, J.O. and M.S.; data curation, P.T.; writing—original draft preparation, J.O. and M.S.; writing—review and editing, P.T.; visualization, J.O.; supervision, J.O.; project administration. All authors have read and agreed to the published version of the manuscript.

Funding: This research was funded by the Growth Project of Young Scientific and Technological Talents of Guizhou Provincial Department of Education (KY [2018]098) and was supported by the Joint Fund of the National Natural Science Foundation of China and the Karst Science Research Center of Guizhou Province (Grant No. U1812401).

Institutional Review Board Statement: Not applicable.

Informed Consent Statement: Not applicable.

Data Availability Statement: No new data were created or analyzed in this study. Data sharing is not applicable to this article.

Acknowledgments: We thank the anonymous reviewers for their constructive and valuable comments and the editors for their assistance in refining this article.

Conflicts of Interest: The authors declare no conflict of interest.

References

- Chen, D.; Rojas, M.; Samset, B.H.; Cobb, A.; Diongue Niang, P.; Edwards, S.; Emori, S.H.; Faria, E.; Hawkins, P.; Hope, P.; et al. Framing, Context, and Methods. In *Climate Change 2021: The Physical Science Basis, Contribution of Working Group I to the Sixth Assessment Report of the Intergovernmental Panel on Climate Change*; Masson-Delmotte, V., Zhai, P., Pirani, A., Connors, S.L., Péan, C., Berger, S., Caud, N., Chen, Y., Goldfarb, L., Gomis, M.I., et al., Eds.; Cambridge University Press: Cambridge, UK; New York, NY, USA, 2021; pp. 147–286.
- Adeel, Z. *Ecosystems and Human Well-Being: Desertification Synthesis: A Report of the Millennium Ecosystem Assessment*; World Resources Institute: Washington, DC, USA, 2005; ISBN 978-1-56973-590-9.
- He, Q. Biotic interactions and ecosystem dynamics under global change: From theory to application. *Chin. J. Plant Ecol.* **2021**, *45*, 1075–1093. [[CrossRef](#)]
- Scheffer, M.; Bascompte, J.; Brock, W.A.; Brovkin, V.; Carpenter, S.R.; Dakos, V.; Held, H.; van Nes, E.H.; Rietkerk, M.; Sugihara, G. Early-warning signals for critical transitions. *Nature* **2009**, *461*, 53–59. [[CrossRef](#)] [[PubMed](#)]
- Alo, C.A.; Wang, G. Potential future changes of the terrestrial ecosystem based on climate projections by eight general circulation models: Future ecosystem changes. *J. Geophys. Res.* **2008**, *113*, G01004. [[CrossRef](#)]
- Bellard, C.; Bertelsmeier, C.; Leadley, P.; Thuiller, W.; Courchamp, F. Impacts of climate change on the future of biodiversity: Biodiversity and climate change. *Ecol. Lett.* **2012**, *15*, 365–377. [[CrossRef](#)] [[PubMed](#)]
- Pearson, R.G.; Dawson, T.P. Predicting the impacts of climate change on the distribution of species: Are bioclimate envelope models useful? Evaluating bioclimate envelope models. *Glob. Ecol. Biogeogr.* **2003**, *12*, 361–371. [[CrossRef](#)]
- Qiao, H.J.; Lin, C.T.; Ji, L.Q.; Jiang, Z.G. mMWeb—An Online Platform for Employing Multiple Ecological Niche Modeling Algorithms. *PLoS ONE* **2012**, *7*, e43327. [[CrossRef](#)] [[PubMed](#)]
- Elith, J.; Leathwick, J.R. Species Distribution Models: Ecological Explanation and Prediction Across Space and Time. *Annu. Rev. Ecol. Evol. Syst.* **2009**, *40*, 677–697. [[CrossRef](#)]
- Ahmed, S.E.; McInerney, G.; O’Hara, K.; Harper, R.; Salido, L.; Emmott, S.; Joppa, L.N. Scientists and software—Surveying the species distribution modelling community. *Divers. Distrib.* **2015**, *21*, 258–267. [[CrossRef](#)]
- Guo, K.Q.; Jiang, X.L.; Xu, G.B. Potential suitable distribution area of *Quercus lamellosa* and the influence of climate change. *Chin. J. Ecol.* **2021**, *40*, 2563–2574. [[CrossRef](#)]
- Pearson, R.G.; Thuiller, W.; Araújo, M.B.; Martinez-Meyer, E.; Brotons, L.; McClean, C.; Miles, L.; Segurado, P.; Dawson, T.P.; Lees, D.C. Model-based uncertainty in species range prediction. *J. Biogeogr.* **2006**, *33*, 1704–1711. [[CrossRef](#)]
- Merow, C.; Smith, M.J.; Silander, J.A. A practical guide to MaxEnt for modeling species’ distributions: What it does, and why inputs and settings matter. *Ecography* **2013**, *36*, 1058–1069. [[CrossRef](#)]

14. Thomas, C.D.; Cameron, A.; Green, R.E.; Bakkenes, M.; Beaumont, L.J.; Collingham, Y.C.; Erasmus, B.F.N.; de Siqueira, M.F.; Grainger, A.; Hannah, L.; et al. Extinction risk from climate change. *Nature* **2004**, *427*, 145–148. [[CrossRef](#)] [[PubMed](#)]
15. Ye, L.Q.; Zhang, W.H.; Ye, X.Z.; Zhang, G.F.; Liu, B.; Ruan, S.N. Prediction of Potential Distribution Area and Analysis of Dominant Environmental Variables of *Davidia involucrate* Based on Maxent. *J. Sichuan Arg. Univ.* **2021**, *39*, 604–612. [[CrossRef](#)]
16. Tan, Y.H.; Zhang, X.J.; Yuan, S.S.; Yu, J.H. Prediction of the ecological suitability of *Gentiana macrophylla* Pall. under scenarios of global climate change. *Chin. J. Ecol.* **2020**, *39*, 3766–3773. [[CrossRef](#)]
17. Feng, L.; Wang, H.Y.; Ma, X.W.; Peng, H.B.; Shan, J.R. Modeling the current land suitability and future dynamics of global soybean cultivation under climate change scenarios. *Field Crops Res.* **2021**, *263*, 108069. [[CrossRef](#)]
18. Brijwal, L.; Pandey, A.; Tamta, S. An overview on phytomedicinal approaches of *Zanthoxylum armatum* DC.: An important magical medicinal plant. *J. Med. Plants Res.* **2013**, *7*, 366–370. [[CrossRef](#)]
19. Editorial Committee of Flora of China. *Flora of China*; Science Press: Beijing, China, 1997; Volume 43, pp. 43–44. ISBN 978-7-03-005486-9.
20. Patade, V.Y.; Kumar, K.; Gupta, A.K.; Grover, A.; Negi, P.S.; Dwivedi, S.K. Improvement in Seed Germination Through Pre-treatments in Timur (*Zanthoxylum armatum* DC.): A Plant with High Medicinal, Economical and Ecological Importance. *Natl. Acad. Sci. Lett.* **2020**, *43*, 295–297. [[CrossRef](#)]
21. Ma, Y.; Fei, X.T.; Li, J.M.; Liu, Y.L.; Wei, A.Z. Effects of location, climate, soil conditions and plant species on levels of potentially toxic elements in Chinese Prickly Ash pericarps from the main cultivation regions in China. *Chemosphere* **2020**, *244*, 125501. [[CrossRef](#)]
22. Chen, L.; Yang, T.X.; Wei, A.Z.; Feng, S.J.; Liu, Y.H. Research Progress on Chinese Prickly Ash. *China Condiment* **2016**, *41*, 149–156. [[CrossRef](#)]
23. Su, J. Investigation and Analysis Report of Chinese Prickly Ash Industry. *Nongjiakaji* **2021**, *1*, 21–25.
24. Phuyal, N.; Jha, P.K.; Prasad Raturi, P.; Rajbhandary, S. *Zanthoxylum armatum* DC.: Current knowledge, gaps and opportunities in Nepal. *J. Ethnopharmacol.* **2019**, *229*, 326–341. [[CrossRef](#)] [[PubMed](#)]
25. Samant, S.S.; Butola, J.S.; Sharma, A. Assessment of diversity, distribution, conservation status and preparation of management plan for medicinal plants in the catchment area of parbati hydroelectric project stage—III in Northwestern Himalaya. *J. Mt. Sci.* **2007**, *4*, 034–056. [[CrossRef](#)]
26. Feng, S.J.; Liu, Z.S.; Hu, Y.; Tian, J.Y.; Yang, T.X.; Wei, A.Z. Genomic analysis reveals the genetic diversity, population structure, evolutionary History and relationships of Chinese pepper. *Hortic. Res.* **2020**, *7*, 158. [[CrossRef](#)] [[PubMed](#)]
27. Feng, S.; Yang, T.; Liu, Z.; Chen, L.; Hou, N.; Wang, Y.; Wei, A. Genetic Diversity and Relationships of Wild and Cultivated *Zanthoxylum* Germplasm Based on Sequence-Related Amplified Polymorphism (SRAP) Markers. *Genet. Resour. Crop Evol.* **2015**, *62*, 1193–1204. [[CrossRef](#)]
28. Nooreen, Z.; Tandon, S.; Yadav, N.P.; Kumar, P.; Xuan, T.D.; Ahmad, A. *Zanthoxylum*: A Review of its Traditional Uses, Naturally Occurring Constituents and Pharmacological Properties. *Curr. Org. Chem.* **2019**, *23*, 1307–1341. [[CrossRef](#)]
29. Zhang, M.; Wang, J.; Zhu, L.; Li, T.; Jiang, W.; Zhou, J.; Peng, W.; Wu, C. *Zanthoxylum Bungeanum* Maxim. (*Rutaceae*): A Systematic Review of Its Traditional Uses, Botany, Phytochemistry, Pharmacology, Pharmacokinetics, and Toxicology. *IJMS* **2017**, *18*, 2172. [[CrossRef](#)]
30. Zhou, T.J.; Zou, L.W.; Chen, X.L. Commentary on the Coupled Model Intercomparison Project Phase 6 (CMIP6). *Clim. Chang. Res.* **2019**, *15*, 445–456. [[CrossRef](#)]
31. Hurtt, G.C.; Chini, L.; Sahajpal, R.; Frothing, S.; Bodirsky, B.L.; Calvin, K.; Doelman, J.C.; Fisk, J.; Fujimori, S.; Klein Goldewijk, K.; et al. Harmonization of global land use change and management for the period 850–2100 (LUH2) for CMIP6. *Geosci. Model Dev.* **2020**, *13*, 5425–5464. [[CrossRef](#)]
32. O'Neill, B.C.; Tebaldi, C.; van Vuuren, D.P.; Eyring, V.; Friedlingstein, P.; Hurtt, G.; Knutti, R.; Kriegler, E.; Lamarque, J.-F.; Lowe, J.; et al. The Scenario Model Intercomparison Project (ScenarioMIP) for CMIP6. *Geosci. Model Dev.* **2016**, *9*, 3461–3482. [[CrossRef](#)]
33. Phillips, S.J.; Anderson, R.P.; Dudík, M.; Schapire, R.E.; Blair, M.E. Opening the black box: An open-source release of Maxent. *Ecography* **2017**, *40*, 887–893. [[CrossRef](#)]
34. Cobos, M.E.; Peterson, A.T.; Barve, N.; Osorio-Olvera, L. kuenm: An R package for detailed development of ecological niche models using Maxent. *PeerJ* **2019**, *7*, e6281. [[CrossRef](#)] [[PubMed](#)]
35. Warren, D.L.; Seifert, S.N. Ecological niche modeling in Maxent: The importance of model complexity and the performance of model selection criteria. *Ecol. Appl.* **2011**, *21*, 335–342. [[CrossRef](#)] [[PubMed](#)]
36. Wang, Y.S.; Xie, B.Y.; Wan, F.H.; Xiao, Q.M.; Dai, L.Y. Application of ROC curve analysis in evaluating the performance of alien species' potential distribution models. *Biodivers. Sci.* **2007**, *15*, 365–372. [[CrossRef](#)]
37. Swets, J.A. Measuring the Accuracy of Diagnostic Systems. *Science* **1988**, *240*, 1285–1293. [[CrossRef](#)]
38. Jiménez-Valverde, A.; Lobo, J.M. Threshold criteria for conversion of probability of species presence to either-or presence-absence. *Acta Oecologica* **2007**, *31*, 361–369. [[CrossRef](#)]
39. Xu, D.P.; Zhuo, Z.H.; Wang, R.L.; Ye, M.; Pu, B. Modeling the distribution of *Zanthoxylum armatum* in China with MaxEnt modeling. *Glob. Ecol. Conserv.* **2019**, *19*, e00691. [[CrossRef](#)]
40. Liu, K.; Nie, G.G.; Zhang, S. Study on the Spatiotemporal Evolution of Temperature and Precipitation in China from 1951 to 2018. *Adv. Earth. Sci.* **2020**, *35*, 1113–1126. [[CrossRef](#)]

41. Hu, M.; Ye, M.; Guo, Y. The Flower Bud Morphological Differentiation and Bud Structure of *Zanthoxylum armatum* DC. *J. Nucl. Agr. Sci.* **2019**, *33*, 1423–1431.
42. Ou, W.F.; Wei, A.Z.; Yang, T.X.; Li, L.X.; Feng, S.J.; Hou, N. Observation and Simulation of the Growth Rules of One-year-old *Zanthoxylum bungeanum* Seedlings from Three Provenances. *J. Northwest For. Univ.* **2016**, *31*, 121–125. [[CrossRef](#)]
43. Zhao, C. *Study on Photosynthetic Characteristics and Low Temperature Stress Physiology of Zanthoxylum armatum*; Sichuan Agricultural University: Chengdu, China, 2018. [[CrossRef](#)]
44. Zhang, H.; Ye, M. Research Status on the Taxonomic and Component of Green *Zanthoxylum bungeanum* Maxim. *North. Hortic.* **2010**, *14*, 199–203.
45. Ma, L.; Yan, H.W.; He, Y.; Zhang, Q.; Liu, B. Vegetation changes in south Himalayas areas based on remote sensing monitoring during 2001–2015. *Arid Land Geogr.* **2017**, *40*, 405–414.
46. Yang, Y.; Dai, X.G.; Wang, P. Projection of Asian Precipitation for the Coming 30 Years and Its Bias Correction. *Chin. J. Atmos. Sci.* **2022**, *46*, 40–54. [[CrossRef](#)]
47. Zhai, Y.J.; Li, Y.H.; Xu, Y. Aridity Change Characteristics over Northern Region of China under RCPs Scenario. *Plateau Meteorol.* **2016**, *35*, 94–106. [[CrossRef](#)]
48. Wu, J.G.; Lv, J.J. Potential effect of climate change on the distribution and range of arid regions. *Res. Environ. Sci.* **2009**, *2*, 199–206. [[CrossRef](#)]
49. Wang, Y.H.; Pei, S.J.; Xu, J.C. Sustainable management of medicinal plant resources in China: Literature review and implications. *Resour. Sci.* **2002**, *24*, 81–88.
50. Meilleur, B.A.; Hodgkin, T. In situ conservation of crop wild relatives: Status and trends. *Biodivers. Conserv.* **2004**, *13*, 663–684. [[CrossRef](#)]
51. Ebert, A.W.; Engels, J.M.M. Plant Biodiversity and Genetic Resources Matter! *Plants* **2020**, *9*, 1706. [[CrossRef](#)]
52. Zhang, X.W.; Jiang, Y.M.; Bi, Y.; Liu, X.L.; Li, X.; Sun, T.; Chen, H.Y.; Li, J. Identification of potential distribution area for *Hippophae rhamnoides* subsp. *sinensis* by the MaxEnt model. *Acta. Ecologica. Sin.* **2022**, *42*, 1420–1428.